The good, the bad and the ugly polishing: Effect of abrasive size on standardless EDS analysis of Portland cement clinker's calcium silicates

Vincent Thiéry, Emmanuel Dubois, Séverine Bellayer

HAL Id: hal-03662917
https://hal.science/hal-03662917

Submitted on 17 Jun 2022

The good, the bad and the ugly polishing: Effect of abrasive size on standardless EDS analysis of Portland cement clinker's calcium silicates

Vincent Thiery [a,b,*], Emmanuel Dubois [c], Séverine Bellayer [d]

[a] IMT Nord Europe, Institut Mines-Télécom, Centre for Materials and Processes, F-59000 Lille, France
[b] Univ. Lille, Institut Mines-Télécom, LGCgE – Laboratoire de Génie Civil et géo Environnement, F-59000 Lille, France
[c] Univ. Lille, CNRS, Centrale Lille, Junia, Université Polytechnique Hauts-de-France, UMR 8520 - IEMN, – Institut d'Electronique de Microélectronique et de Nanotechnologie, F-59000 Lille, France
[d] Univ. Lille, CNRS, INRAE, Centrale Lille, UMR 8207 - UMET - Unité Matériaux et Transformations, F-59000 Lille, France

ARTICLE INFO

ABSTRACT

Standardless Energy dispersive spectroscopy (EDS) on polished samples of Portland cement clinker is routinely performed both for unhydrated phases as well as in cement pastes. Typically, the calcium to silica ratio is investigated. EDS analyses are highly dependent on the polishing quality of the sample. It is thus worth studying the Ca/Si ratios of cement phases in a clinker since they can be used as a reference. Indeed, alite (Ca_3SiO_5 or C_3S in cement chemistry notation) and belite (Ca_2SiO_4 or C_2S) should have an atomic Ca/Si ratio of 3 and 2, respectively. EDS carried out under the scanning electron microscope (SEM) is routinely used on polished samples to assess the composition of such phases. In the present study, Ca/Si ratios are investigated on a commercial clinker polished at various steps (6, 3, 1 and 0.25 μm diamond pastes, 0.05 μm alumina). All along the polishing process, ratios are coherent with theoretical ones and with the reference ones obtained by electron probe microanalysis (EMPA) in the present study.

1. Introduction

1.1. Cementitious materials: microstructure and polishing

The microstructural study of cementitious materials is most of the time carried out with a scanning electron microscope (SEM) using flat polished samples or fractures (Famy et al., 2002; Scrivener, 2004; Stutzman, 2012, 2004). Flat-polished samples offer a cross-section through the sample and allow microanalysis, typically energy dispersive spectroscopy (EDS), which is the most commonly used analytic technique for cement and concrete (Pacheco and Çopuroğlu, 2016; Richardson and Groves, 1993; Wong and Buenfeld, 2006), but also supplemented in some cases by wavelength dispersive spectroscopy (WDS), commonly known as electron microprobe analyser or EMPA (Ghose et al., 1983; Ghose and Barnes, 1979; Rayment, 1986; Sarkar and Roy, 1985; Staněk and Sulovský, 2015, 2012).

Samples to be studied as polished cross-sections are prepared by epoxy impregnation (Kjellsen et al., 2003; Marusin, 1995) followed by several steps of polishing. The mechanisms of polishing, consisting of a removal of matter in order to suppress surface imperfections, are

complex (Evans et al., 2003), depend on the type of material to be polished and have an influence on the result of microanalysis (Newbury and Ritchie, 2015; Rémond et al., 2006).

There is no normative, well-defined procedure for the polishing of cement-based materials, but only common practice. This one is sometimes contradictory between papers and is totally user dependent. Nowadays, most publications mention the use of diamond-based products, but some works refer to alumina (Ahmed, 1983) or cerium oxide (Jupe et al., 2012) for example.

EDS microanalysis is strongly dependent on the flatness of the analysed surface, the slightest angle between the place analysed and the electron beam will have a strong effect on results – this matter has already been extensively studied (Newbury and Ritchie, 2015, 2013; Yakowitz, 1968). EDS is not a surface science technology, the size of the electron-matter interaction zone exceeding a diameter of 1 μm, even sometimes more in the case of porous cementitious materials (Kjellsen and Helsing Atlassi, 1998; Wong and Buenfeld, 2006). However, since polishing can leave surface imperfections, the accuracy of analyses is questionable. Indeed, considering the presence of scratches, the X-ray path resulting from the interaction between the incident electron beam
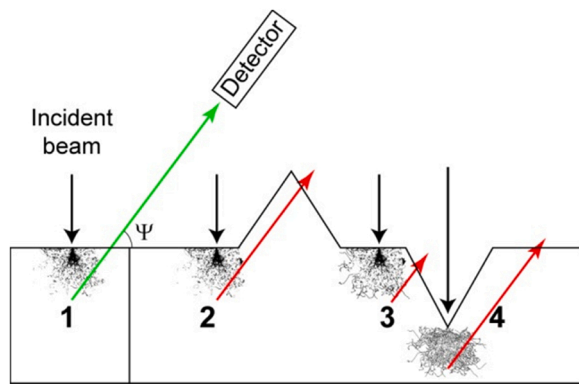
Fig. 1. Redrawn after Newbury and Ritchie (2013): schematic cross section through a sample showing the topographic effect of the X-ray path and thus on microanalysis. 1: flat area with a correct geometry, yielding accurate results. 2: extra absorption due to ridge. 3: reduced absorption due to scratch wall. 4: extra absorption path due to scratch depth.

and the sample is likely to be affected (Fig. 1).

Even though calcium silicate in Portland cement clinker has been well known for decades, their microanalysis is still of interest nowadays. EDS can be performed for example as an educational tool in order to illustrate Ca/Si ratios or in routine quality control as well as when incorporating various foreign elements in belite (Staněk and Sulovský, 2012).

Moreover, the quantitative microstructural study of cement paste, and more specifically the pore structure, is likely to be affected by nanometric changes in surface inclination (Yio et al., 2016). This is typically what happens on a poorly polished surface.

1.2. Chemistry of calcium silicates

Being important phases in both cement and ceramic sciences, the chemistry and crystallography of Ca_2SiO_4 ("calcium orthosilicate") and Ca_3SiO_5 (tricalcium silicate) is described in a large amount of papers (Ghosh et al., 1979; Maki, 2006a, 2006b; Taylor and Aldridge, 1993; Yamnova et al., 2011). Published data concerns both the naturally occurring minerals (larnite and hatrurite) as well as their synthetic counterparts (Table 1).

The present study provides analyses of Portland cement clinker's calcium silicates, alite (Ca_3SiO_5 or C_3S) and belite (Ca_2SiO_4 or C_2S) on polished samples at each fine polishing step. In order to have a reference for phase composition of clinker samples from the present study, di- and tri-calcium silicates compositions have been also investigated by

electron probe microanalysis (EPMA). The microstructure is investigated using common techniques (optical microscopy – OM – and scanning electron microscopy – SEM) completed by optical profilometry to obtain a quantitative image of surface defects. The reason for this choice is that the Ca/Si atomic ratio for those two components can be used as a basis for comparison between the successive steps of polishing. Finally, to go further, a brief study on a pure cement paste is also presented since its EDS microanalysis under the SEM is routinely done by plotting Ca/Si ratios (Georget et al., 2021; Sargam and Wang, 2021).

1.3. Surface metrology

The arithmetic mean roughness, R_a along a line is defined as (equation 1):

$$R_a = \frac{1}{n} \sum_{i=1}^{n} |y_i| \tag{1}$$

Arithmetic mean roughness.

It can be viewed as the measurement of n points of height y_i, the spacing being the spatial sampling used for the measurement. With a nanometric resolution, this device is typically used to study defects on highly polished surfaces for example (Awasthi et al., 2021), to quantify micro grinding tools roughness (Setti et al., 2019) as well as enamel

Table 2
Summary of all polishing steps for the samples analysed in this study. See text for details regarding lubricants. All steps have been carried out at 150 rpm with a 25 N load except for lapping which was carried out slower.

	Abrazise size	Type	Duration
Coarse polishing	80 grit	Resin-embedded diamond	Until sample crops out
	220 grit	Resin-embedded diamond	10 s
	600 grit	Resin-embedded diamond	30 s
	1200 grit	Resin-embedded diamond	60 s
Lapping	800 grit	SiC suspension in ethanol on a pig iron plate	6 min
Fine polishing	6 µm	Diamond paste on cloth (Struers DP Dac)	5 min
	3 µm	Diamond paste on cloth (Struers DP Dac)	5 min
	1 µm	Diamond paste on cloth (Struers DP Dac)	5 min
	0.25 µm	Diamond paste on cloth (Struers DP Dac)	5 min
	0.05 µm	Alumina slurry on cloth (Struers DP Dac)	20 s

Table 1
Chemistry of calcium silicates. (1) Theoretical Ca_2SiO_4, (2) after (Midgley and Bennet, 1971), (3) after (Sarkar and Roy, 1985), (4) theoretical Ca_3SiO_5, (5) after (Gross, 1977), (6) after (Sarkar and Roy, 1985). (2), (3), (5) and (6) are electron microprobe (WDS) analysis.

	Larnite – Ca_2SiO_4 or C_2S			Hatrurite – Ca_3SiO_5 or C_3S		
	(1)	(2)	(3)	(4)	(5)	(6)
CaO	65.12	65.5	64.45	73.69	72.8	71.80
SiO_2	34.88	34	29.03	26.31	26.1	23.17
MgO		0.05	0.70		Traces	0.39
Al_2O_3		0.03	1.85		0.4	1.48
K_2O		0.037	0.79			0.79
Na_2O		0.25	0.78			0.70
TiO_2		0.029	0.11		0.3	0.40
MnO		0.074			0.2	
MnO_2			0.25			0.13
Fe_2O_3		0.011	1.65			1.24
P_2O_5		0.48	0.52			0.24
SO_2		0.057				
SO_3			0.23			0.36
Cr_2O_3			0.13			0.15
Total	100	100.52	100.49	100	99.8	100.84

Objective	Lateral resolution	Vertical resolution
x 10	0.9 μm	< 0.1 nm
x 50	0.5 μm	< 0.1 nm

demineralization (Cross et al., 2009). This versatile tool is thus of interest to study the polishing of cement-based materials in cases where a sub-micrometric information is needed.

2. Materials and methods

2.1. Sample embedding and polishing

In scanning electron microscopy, it is well established that a correct sample preparation is the key to relevant observations (Kjellsen et al., 2003; Scrivener et al., 2016). A commercial Portland clinker (courtesy of Lafarge-Holcim) was used for this study. Centimetre sized nodules were halved prior to impregnation in order to obtain the largest possible surface of observation. Impregnation was carried out under vacuum at ambient temperature using epoxy resin (K2020, Huntsman). A summary of all polishing steps is given in Table 2. A mixed alcohol-oil lubricant (DP Brown, Struers) was used for all steps except for the coarse polishing and lapping carried out with ethanol only.

2.2. Imaging, scanning electronic microscopy and microanalysis

Optical images were acquired with a Leica DMRXP microscope coupled with the Leica LAS software. Scanning electron microscopy was carried out using a Hitachi S-4300SE/N SEM working in high vacuum mode, coupled to a Thermoscientific Ultradry EDX SDD detector. The beam current was set to 15 kV with a time constant of 8 μs in order to keep a deadtime in the 10–20% range. Data were processed using Noran System Six software, choosing a standardless method with ZAF
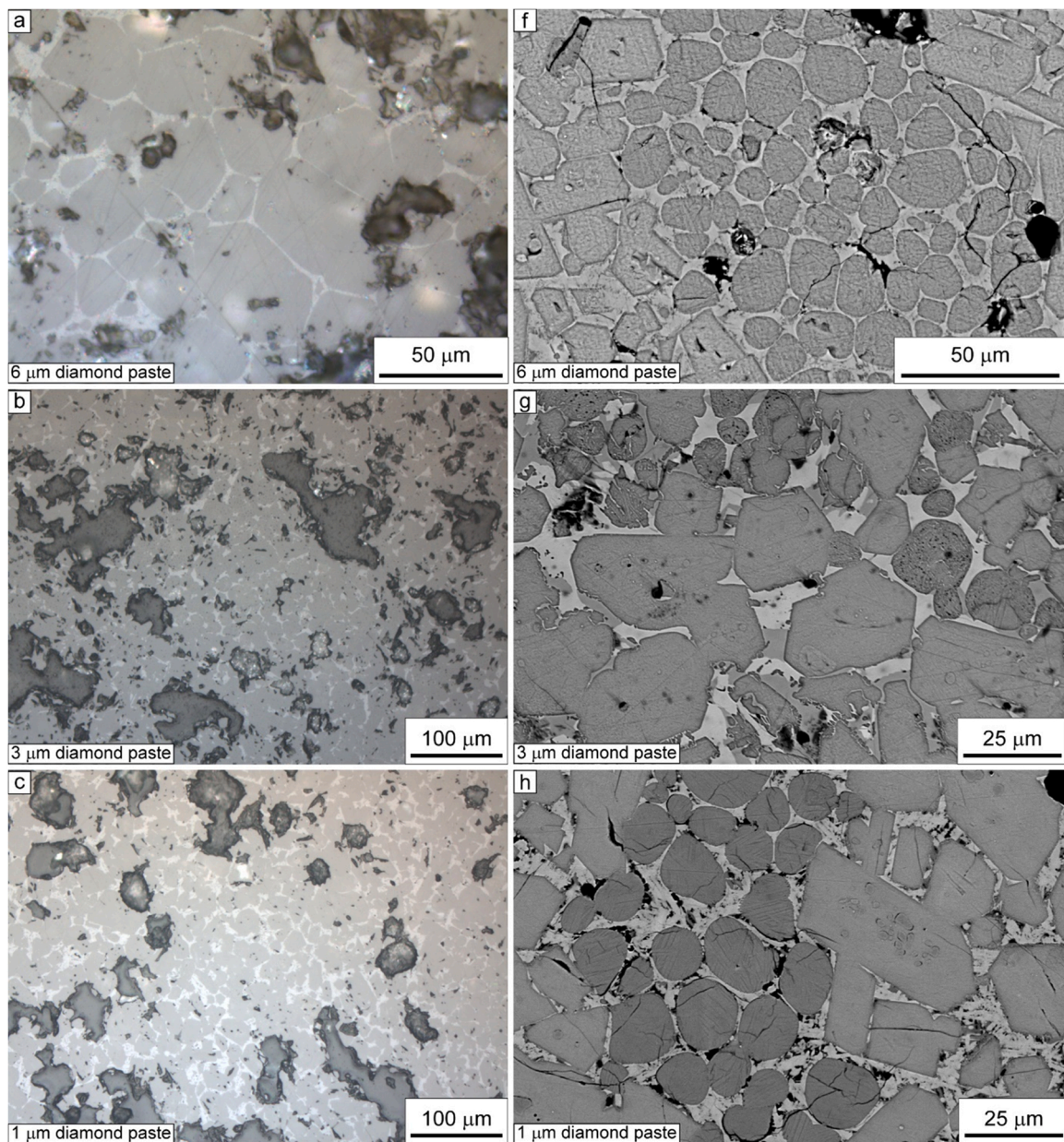

Fig. 2. Optical (a-c) and SEM-BSE (f-h) micrographs illustrating the evolution of the polishing at successive steps Optical (d-e) and SEM-BSE (i-j) micrographs illustrating the evolution of the polishing at successive steps.
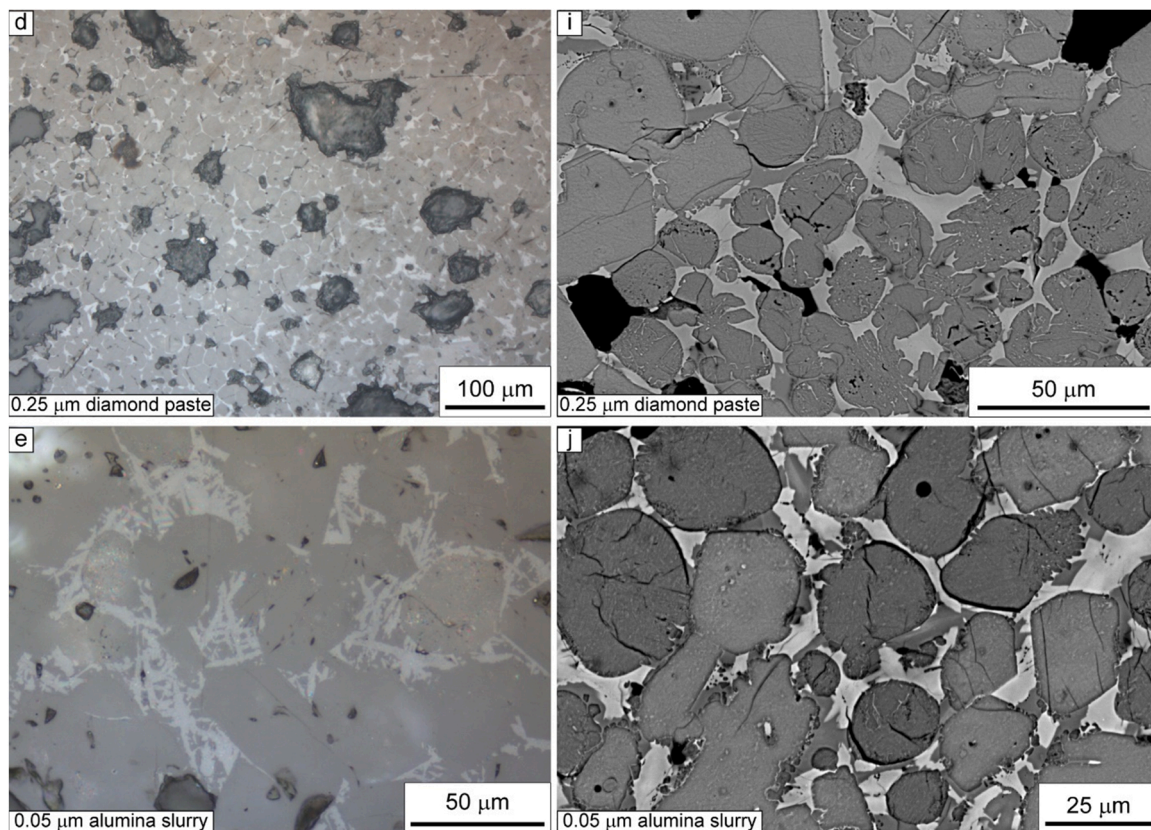
Fig. 2. (*continued*).

correction.

2.3. Electron probe microanalysis

A Cameca SX100 electron probe microanalyser (EPMA) was used to perform quantitative elemental analysis. Quantifications were carried out at 15 kV, 15 nA. The acquisition time was set at 20 s per element. A LLiF crystal was used to detect the Fe Kα X-rays, a LPET crystal to detect the Ca, P, S and K Kα X-rays and a TAP crystal to detect the Si, Al, Na and Mg Kα X-rays. The standards used to quantify Si, Ca, Al, K, Fe, P, S, K, Na and Mg were, respectively, wollastonite, orthose, Fe2O3, apatite, ZnS, albite and MgO.

2.4. Optical profilometry

A Bruker Contour GT-X optical profiler, working in vertical scanning interferometry (VSI) mode under white light, was used on polished samples to obtain their surface topography. The main characteristics of the objectives used in the present study are presented in Table 3.

3. Results

3.1. Microstructure

3.1.1. Polishing - 6 μm step

From this step, the microstructure is optically revealed (Fig. 2a). Under the SEM-BSE, it is clear but not perfect. The surface of calcium silicates is rough, and the interstitial phase is not differentiated. Scratches are numerous. It is worth noting that the inner structure of the C_2S, the so-called "striation" or lamellae (Chromy, 1967; Fukuda and Maki, 1989), is not decipherable. It even appears overprinted by scratches on SEM images.

3.1.2. Polishing - 3 μm and subsequent steps

Since the microstructure has been revealed from the 6 μm step, no deep changes are expected from this point. The main improvement concerns the scratches, which are not visible under the optical microscope, but they are still present at some places as revealed by the SEM (Figure b and c). The changes after the 1 μm step are not easily seen on micrographs but rather under optical microscopy since the sample is more reflective.

3.1.3. EMPA microanalysis (standard-based)

In mineralogical studies, especially in geosciences, EMPA, based on the measurement of the wavelength of the emitted X-rays (WDS: wavelength dispersive spectroscopy) is usually preferred to EDS (energy dispersive spectroscopy) for its lower limits of detection and higher spectral resolution (Reed, 2005). While EDS has proved to be as effective as WDS in some cases (Gauvin, 2012), the latter remains a reference in microanalysis of minerals. It had been however poorly used to characterize clinker phases (Rayment and Majumdar, 1994; Sarkar and Roy, 1985; Staněk and Sulovský, 2015).

Within the present study, alite (tricalcium silicate) and belite (dicalcium silicate) have been analyzed by EPMA (WDS) as a complement to EDS analysis, which is presented below. The measurement has been done on optically polished samples as described above. Table 4 presents the data expressed in w*r*.% and as calculations of structural formula.

Disregarding all impurities, belite has a structural formula of $Ca_{1,94}Si_{0,94}O_4$ (mean over ten analyses), which gives a Ca/Si ratio of 2,06 and alite $Ca_{2,7}Si_{0,9}O_5$ (mean over ten analyses), which gives a Ca/Si ratio of 3. Both are in good agreement with theoretical valued for pure phases and the amount and nature of foreign ions are also coherent with what has been described elsewhere (Maki, 2006a, 2006b; Taylor, 1997).

Table 4

EPMA (WDS) microanalysis for belite (C_2S) and alite (C_3S) of the studied clinker.

Ca_2SiO_4 – Belite – wt%

Na_2O	MgO	SiO_2	Al_2O_3	CaO	P_2O_5	SO_2	K_2O	FeO	Total
0,31	0,53	32,24	0,72	59,54	0,12	0,08	0,64	0,52	94,70
0,47	0,63	31,24	1,40	61,54	0,12	0,19	0,64	0,99	97,23
0,37	0,65	31,14	2,03	60,40	0,13	0,22	0,63	1,02	96,59
0,67	0,45	28,79	1,23	60,37	3,71	0,11	1,29	0,66	97,29
0,34	0,50	31,74	1,21	61,04	0,13	0,26	0,62	0,77	96,61
0,34	0,55	31,56	1,35	61,31	0,08	0,28	0,57	0,89	96,92
0,56	0,75	31,44	1,78	58,95	0,14	0,29	0,76	0,88	95,55
0,57	0,72	31,84	1,21	61,11	0,11	0,25	0,68	0,88	97,38
0,20	0,48	33,59	0,32	62,11	0,20	0,03	0,45	0,45	97,82
0,22	0,53	33,44	0,48	61,95	0,08	0,03	0,52	0,66	97,90

Atoms per formula unit based on 4 oxygen

Na	Mg	Si	Al	Ca	P	S	K	Fe	
0,02	0,02	0,98	0,03	1,93	0,00	0,00	0,02	0,01	
0,03	0,03	0,93	0,05	1,97	0,00	0,01	0,02	0,02	
0,02	0,03	0,93	0,07	1,93	0,00	0,01	0,02	0,03	
0,04	0,02	0,85	0,04	1,91	0,09	0,00	0,05	0,02	
0,02	0,02	0,95	0,04	1,95	0,00	0,01	0,02	0,02	
0,02	0,02	0,94	0,05	1,96	0,00	0,01	0,02	0,02	
0,03	0,03	0,95	0,06	1,90	0,00	0,01	0,03	0,02	
0,03	0,03	0,94	0,04	1,94	0,00	0,01	0,03	0,02	
0,01	0,02	0,99	0,01	1,95	0,00	0,00	0,02	0,01	
0,01	0,02	0,98	0,02	1,95	0,00	0,00	0,02	0,02	

Ca_3SiO_5 – Alite – wt%

Al_2O_3	MgO	SiO_2	Al_2O_3	CaO	P_2O_5	SO_2	K_2O	FeO	
0,08	1,35	24,99	0,73	69,05	0,11	0,01	0,05	0,58	96,95
0,07	1,40	24,32	1,09	69,24	0,14	0,04	0,09	0,64	97,04
0,08	1,35	24,95	0,79	69,58	0,15	0,01	0,06	0,60	97,58
0,10	1,43	24,41	1,24	69,28	0,07	0,04	0,08	0,83	97,46
0,11	1,27	25,57	1,03	68,61	0,11	0,04	0,13	0,72	97,58
0,09	1,35	24,63	0,85	69,08	0,13	0,01	0,06	0,59	96,79
0,08	1,40	24,56	0,82	68,81	0,28	0,01	0,09	0,65	96,69
0,09	1,45	24,31	1,15	68,16	0,14	0,02	0,06	0,80	96,18
0,11	1,33	24,81	0,77	68,37	0,19	0,02	0,06	0,54	96,20
0,09	1,43	24,00	1,30	68,05	0,17	0,04	0,12	0,79	96,00

Atoms per formula unit based on 5 oxygen

Na	Mg	Si	Al	Ca	P	S	K	Fe	
0,01	0,07	0,92	0,03	2,71	0,00	0,00	0,00	0,02	
0,01	0,08	0,89	0,05	2,72	0,00	0,00	0,00	0,02	
0,01	0,07	0,92	0,03	2,73	0,00	0,00	0,00	0,02	
0,01	0,08	0,90	0,05	2,72	0,00	0,00	0,00	0,03	
0,01	0,07	0,94	0,04	2,70	0,00	0,00	0,01	0,02	
0,01	0,07	0,90	0,04	2,71	0,00	0,00	0,00	0,02	
0,01	0,08	0,90	0,04	2,70	0,01	0,00	0,00	0,02	
0,01	0,08	0,89	0,05	2,68	0,00	0,00	0,00	0,02	
0,01	0,07	0,91	0,03	2,69	0,01	0,00	0,00	0,02	
0,01	0,08	0,88	0,06	2,67	0,01	0,00	0,01	0,02	

3.2. EDS standardless microanalysis

3.2.1. Effect of X-rays counts amount on the quality of the data

Counting time is a useless parameter; the analysis had to be monitored as the amount of X-rays detected. Typically, 10 000 counts above the background level is recommended (Newbury and Ritchie, 2013). It can be seen in Fig. 3 that the overall spectra shape as well as the Ca/Si ratio (Table 4) are obtained as early as 100 counts only are reached. EDS spectra become smoother when more counts are recorded but there is no significant change in the analytical results (Table 2 for alite, Table 3 for belite) – however, it must be stated that the associated error is divided by ten when the amount of counts increases.(Tables 5 and 6).

3.2.2. Semiquantitative results

For each sample, i.e., a clinker at various polishing steps, 50 points of analysis were taken randomly on the two types of calcium silicates. The results are summarized in Fig. 4 and Table 7. Analytical values are given as supplementary materials. Some dubious points (e.g. Ca/Si ratio of 8) have been removed manually.

The graphical representation is helpful to see the variations. For belite (C_2S), the theoretical Ca/Si ratio of 2 is constantly a bit overestimated (2.1–2.2) except after the 0.25 μm step (2.05). For the C_3S, the tendency is opposed as the Ca/Si value of 3 is reached as early as the 6 μm step and has a significant change only after the 0.25 μm step. The Ca/Al ratio is plotted only to have a basis for comparison, the scattering is due to compositional effect, i.e. a variation in Al content, noticeable especially in C_2S, which has already been described (Harrisson et al., 1985).

In order to check the statistical relevance of those observations, a preliminary analysis of variance (anova test) was carried out for both C_2S and C_3S Ca/Si ratios at various steps of polishing. The results for C_2S reveals that the F factor (25,24) is superior to F_{crit} (2.41) thus the null hypothesis (all means are equal) is false. This is the same for C_3S where F (62.64) > F_{crit} (2.41). Hence, a t-test has to be carried out (Table 8). The global trend is that t-factors are low and tend to drastically diminish with the polishing, indicating that this one has no significant effect on the data. There is one noticeable exception, which has no explanation: for C_2S at the 1 to 0,25 μm step the t-factor is several orders of magnitude greater that for C_3S.
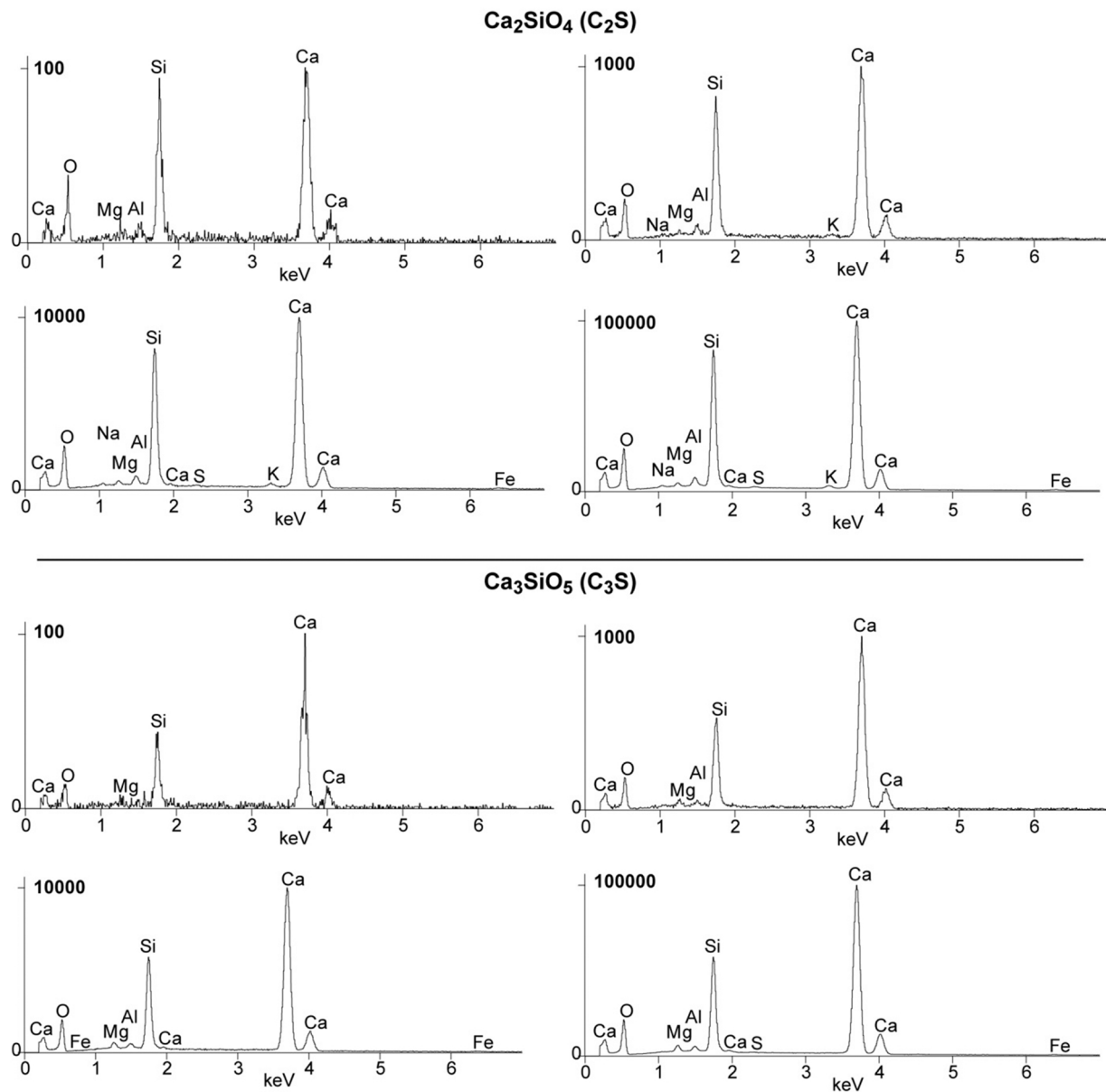
Ca₂SiO₄ (C₂S)

Ca₃SiO₅ (C₃S)

Fig. 3. Effect of the amount of X-rays count on di- and tri-calcium silicates EDS spectra.

Table 5
Influence on the amount of counts (Ca Kα1) on the Ca/Si ratio of alite (C₃S) and corresponding error.

| Numbre of counts	O	O error	Na	Na error	Mg	Mg error	Al	Al error	Si	Si error	Ca/Si	Ca/Si error (2σ)
100	39	12,1	0,5	0,9	1	0,7	0,4	0,5	14,3	1,8	3,08	0,64
1,00E+ 03	47,1	2,9	1	0,2	1,2	0,2	0,9	0,1	12,1	0,4	3,04	0,16
1,00E+ 04	48	1	0,5	0,1	1,1	0,1	0,9	0	12	0,1	3,08	0,05
1,00E+ 05	48	0,5	0,6	0	1,4	0	1,1	0	12	0,1	3,01	0,04
	P	**P error**	**S**	**S error**	**K**	**K error**	**Ca**	**Ca error**	**Fe**	**Fe error**		
	0,1	0,7	0,4	0,6	0,1	0,6	44,1	3,4	0,2	1,6		
	0,4	0,1	0,1	0,1	0,3	0,1	36,8	0,7	0,1	0,1		
	0,2	0	0,2	0	0,2	0	36,9	0,3	0	0,1		
	0,4	0	0,2	0	0,2	0	36,1	0,2	0	0		

3.3. Optical profilometry

Even though the microstructure is revealed and analytical values for Ca/Si atomic ratios are coherent with theoretical values, it is of interest to characterize the smoothness of a polished surface. Optical profilometry allows measurement of surface irregularities with a nanometric resolution (Fig. 5 and Table 9) and provides a 3D reconstruction to highlight them.

The surface after the 6 μm step does not show any polishing reliefs between phases. The only differences are porosities which are poorly filled with resin and numerous scratches. This is in good agreement with what has been observed with both OM and SEM. Holes are up to 4 μm

Table 6
Influence on the amount of counts (Ca Kα1) on the Ca/Si ratio of belite (C₂S) and corresponding error (2 σ).

Number of counts	O	O error	Na	Na error	Mg	Mg error	Al	Al error	Si	Si error	Ca/Si	Ca/Si error
100	45,4	8,5	1	0,7	0,8	0,4	1,6	0,5	16	1,3	2,14	0,31
1,00E+ 03	46,9	2,6	1	0,2	0,9	0,1	1,5	0,1	15,2	0,4	2,16	0,10
1,00E+ 04	49,1	0,9	0,8	0,1	0,7	0	1,2	0	14,9	0,2	2,16	0,05
1,00E+ 05	47,1	0,5	1,5	0	1	0	1,6	0	15,1	0,1	2,11	0,03
	P	**P error**	**S**	**S error**	**K**	**K error**	**Ca**	**Ca error**	**Fe**	**Fe error**		
	0,4	0,3	0,3	0,3	0,1	0,3	34,3	2,1	0,1	0,8		
	0,4	0,1	0,3	0,1	0,6	0,1	32,9	0,6	0,3	0,2		
	0,1	0	0,3	0	0,6	0	32,2	0,3	0,2	0,1		
	0,5	0	0,5	0	0,7	0	31,8	0,2	0,3	0		
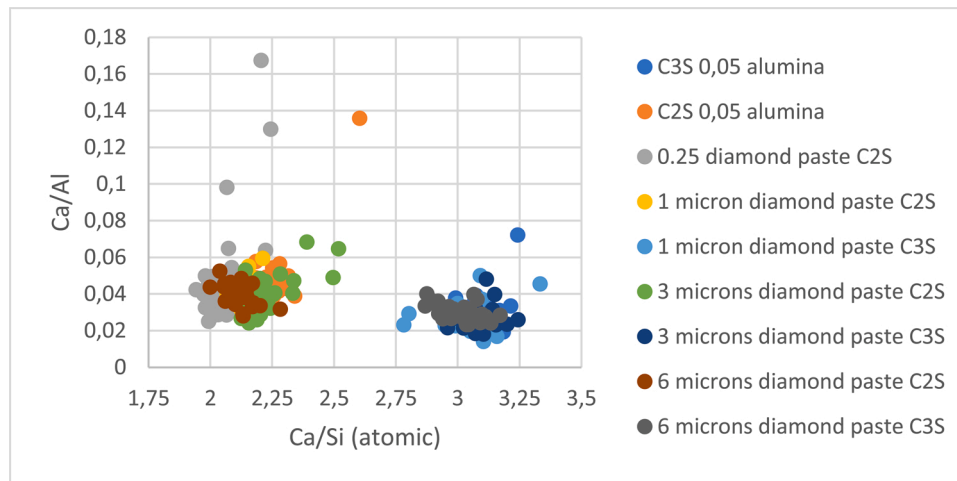
Fig. 4. Ca/Al vs. Ca/Si atomic plots at the various steps of polishing.

Table 7
Evolution of the Ca/Si ratio of belite (C₂S) and alite (C₃S) and corresponding error (2 σ).

	Polishing Step				
	6	3	1	0.25	0.05
C₂S	2.13 ± 0.08	2.21 ± 0.08	2.15 ± 0.08	2.06 ± 0.08	2.25 ± 0.08
C₃S	3.01 ± 0.11	3.06 ± 0.12	3.04 ± 0.14	2,88 ± 0.11	3.08 ± 0.13

Table 8
Results of the t-test for Ca/Si ratios during the evolution of polishing.

	Ca/Si from 6 to 3	Ca/Si from 3 to 1	Ca/Si from 1–0.25	Ca/Si from 0.25 to 0.05
C₂S	1,5 E-03	1,0 E-03	9,0 E-03	5,2 E-19
C₃S	3,5 E-04	4.6 E-02	7,8 E-16	1,7 E-19

deep, maybe even more but they have not been investigated since they are not likely to be places of analyses. Regarding scratches, they are present almost everywhere on the surface. They are typically 100–200 nm deep according to the profiles obtained (Fig. 5).

After the 3 μm polishing step, the surface is remarkably smooth, confirming what has been observed in OM and SEM while no scratches are to be seen. Surface irregularities are of a few tenth of nanometers. It is worth noting that there are no polishing irregularities between phases, namely, the two types of silicates and the interstitial phase. The same observation can be done after the 1 μm polishing step which is even smoother, without any polishing irregularities at phase boundaries.

An interesting phenomenon occurs once the 0.25 μm step is reached. While the interstitial phase was previously undecipherable between silicate grains, it appears a bit above them, meaning that it is more resistant to abrasion.

This irregularity is even more marked after the 0.05 μm polishing step. In both cases, those steps between phases are not exceeding 100 nm in height.

4. Perspectives towards cement paste

Since SEM-EDS statistical studies on the composition of cement pastes are classically done (Georget et al., 2021), the application of the previous steps of the present study are relevant to ensure data quality. Thus, in order to have also an insight on the polishing quality of a cement paste, a pure paste with a water/cement ratio of 0.5 (see protocol for paste preparation in Maimouni et al., 2018) optically correctly polished, has been characterized by optical profilometry (Fig. 7).

While the microstructure seems optically correctly polished and its appearance under the SEM corresponds to what is expected from a cementitious microstructure, the optical profilometer reveals the extent to which extent surface defects are present. As it can be expected, the zones with the highest polishing elevation are the ones corresponding to anhydrous clinker remnants within the hydrated paste. The R_a parameter is of 91.3 nm, which is in the same order of magnitude as the results obtained on pure clinker phases.

5. Discussion and perspectives

5.1. Monitoring the polishing quality with optical profilometry

The use of optical profilometry is an interesting complement to optical or electron micrographs when it comes to the fine study of microstructure. While SEM alone can be used to perform topographic characterization (Ersoy et al., 2008; Limandri et al., 2016), there are some uncertainties, especially at low magnifications (Kang et al., 2012).
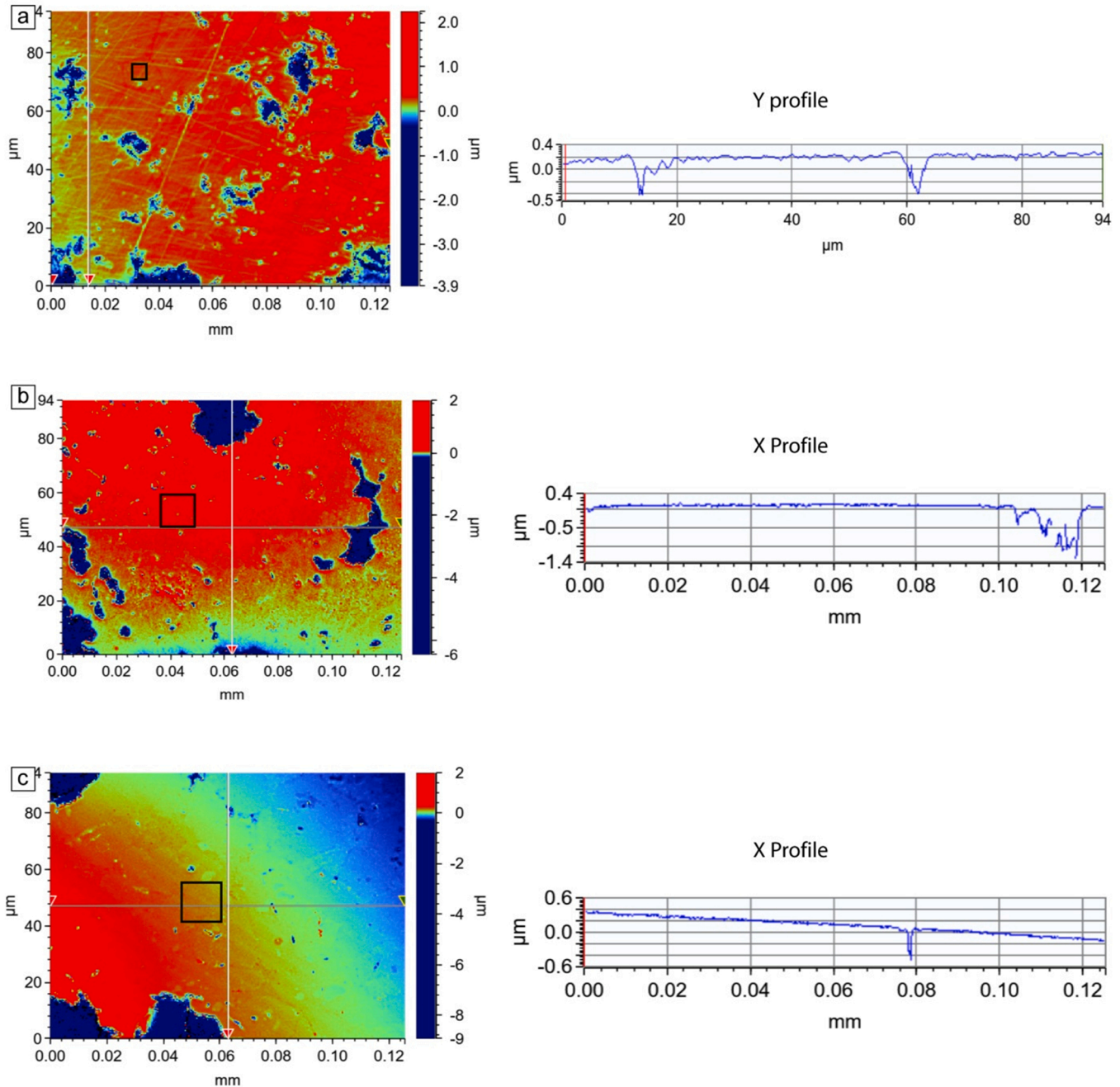
Fig. 5. Height maps (left) and associated topographic profiles (right) for 6 (a), 3 (b) and 1 (c) μm polishing steps, obtained by optical profilometry without levelling due to surface tilt. The black squares indicate the zones where the Ra parameter has been calculated. The profile presented in c is inclined because of a lack of parallelism between the faces of the polished section.

Table 9
Ra parameter for polished surface of clinker at various polishing steps.

Abrasive size (in μm)	Ra (nm)
6	53.2 (inside a C_2S)
3	103
1	160
0.25	140 (inside a C_2S)
0.05	181 (inside a C_2S)

Based on height maps and topographical profiles (Figs. 5 and 6) and micrographs (Fig. 2), it appears that surface defects of some tenth, even 100–200 nm, have no significant influence on the EDS results. Indeed, Ca/Si ratios for C_2S and C_3S are close to theoretical values from the moment the microstructure is revealed (i.e. after the 6 μm polishing step).

It must be reminded that calcium silicates from Portland cement clinker are not pure phases since many substitutions are possible. Indeed, Taylor (1997) proposed the following structural formulas:

Belite or C_2S $(K_{0,01}Na_{0005}Ca_{0975}Mg_{0,01})_2(Fe_{0,02}Al_{0,06}Si_{0,90}P_{0,01}S_{0,01})O_{3,96}$ which gives a Ca/Si atomic ratio of 2,16,
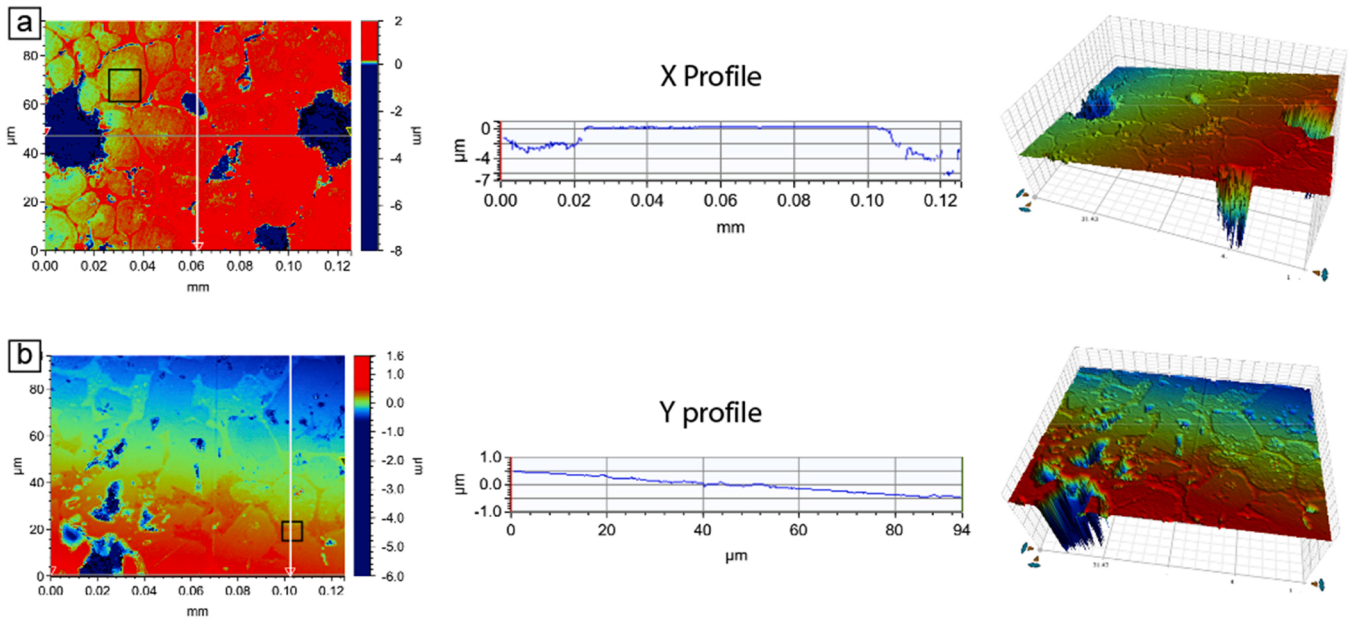
Fig. 6. Height maps (left), associated topographic profiles (center) and 3D models (right) for (a) 0.25 μm and (b) 0.05 μm polishing steps, obtained by optical profilometry without levelling due to surface tilt.
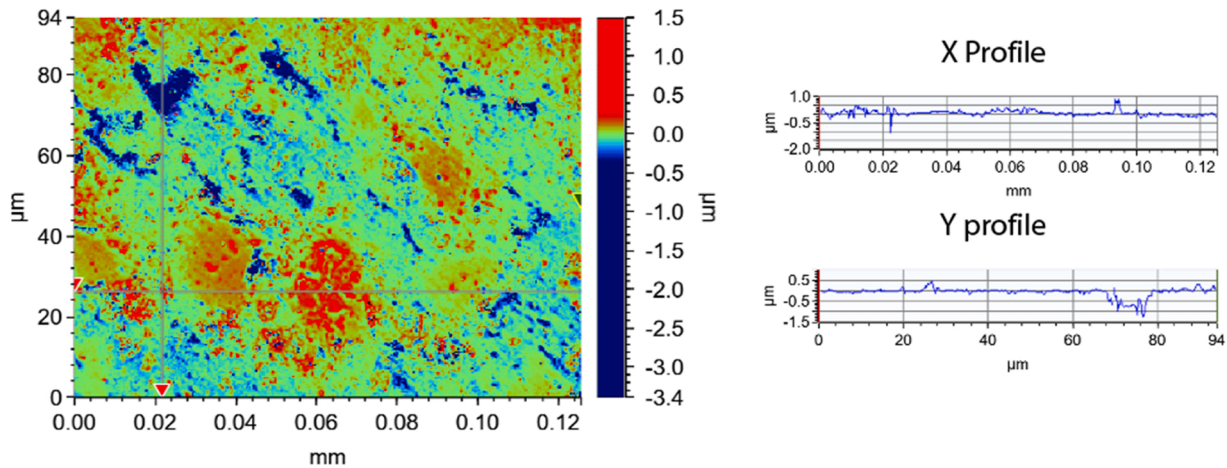

Fig. 7. Optical profilometry elevation map of a pure cement paste and associated profiles.

Alite or C_3S $(Ca_{0.98}Mg_{0.01}Al_{0067}Fe_{0,0033})_3(Si_{0,97}Al_{0,03})O_5$ which gives a Ca/Si atomic ratio of 3,03·

The new data of the present study (Table 4) is in good agreement with those values.

Here, only diamond-based abrasives have been used, except for the last polishing step (0.05 μm alumina). Some authors have illustrated (Newbury and Ritchie, 2015) up to 0.8 wt% of difference in analyses for some elements (Mg in their case). It does not seem that this abrasive has a significant impact on the analysis of calcium silicates.

Flat polished samples are not used only for optical microscopy or SEM-EDS characterization. They are also of tremendous importance in nanoindentation studies (Velez et al., 2001), for which surface requirements are high and polishing steps are likely to be very long, reaching several hours (Miller et al., 2008). Thus, a sample polished for SEM-EDS is likely to yield accurate results easily since the polishing steps presented here (Table 2) can be performed in less than one hour but might be useless for a correct indentation study.

It has been shown that EDS analysis can be influenced by the crystallographic orientation of the material analyzed (Bourdillon et al., 1981). In a clinker nodule, crystal orientation is not obvious (Rößler

et al., 2017), nor in clinker relics of aged cementitious materials (Secco et al., 2014), as revealed by electron backscattered diffraction (EBSD). Hence, since the material is crystallographically heterogeneous, it is likely that random EDS analysis on a wide amount of crystals is likely to display some changes but it remains to be demonstrated. It is worth noting that EBSD is also dependent on the good quality of the polishing, the interaction between the electron beam and the sample occurring at depths in the 50–100 nm range (Nowell et al., 2005).

5.2. Standard vs. standardless analysis

The debate about quantitative analysis using EDS under the SEM (instead of WDS) is almost settled (Gauvin, 2012; Newbury and Ritchie, 2015, 2013; Ritchie et al., 2012). However, there does not seem to be any published data relative to the use of standard-based analysis on cementitious materials (exception made of the aforementioned WDS characterization of calcium silicates), and most of the published work does not provide enough details regarding analytical conditions. Studies based on large EDS sets of data are typically based on ratios (Famy et al.,

2003; Georget et al., 2021).

Data obtained by WDS (EMPA) give a Ca/Si mean ratio of 2,06 for belite and 3,00 for alite (10 analysis for both silicates), which are almost as identical as theoretical ratios and very close to the ones obtained by standardless EDS.

6. Conclusion

As a conclusion, it can be stated that once the microstructure is revealed, providing that EDS analyses are not performed in polishing pits, wide scratches or porosities, semi-quantitative results are likely to be correct. However, the slightest defect in polishing can result in misconceptions during the study of the microstructure by tools such as nanoindentation or EBSD.

Compliance with ethical standards

The authors declare that they have no conflict of interest.

Declaration of Competing Interest

The authors declare that they have no known competing financial interests or personal relationships that could have appeared to influence the work reported in this paper.

Acknowledgements

Appendix A. Supporting information

Supplementary data associated with this article can be found in the online version at doi:10.1016/j.micron.2022.103266.

References

Ahmed, W.U., 1983. Improvements in Samples Preparation Technique for Microscopic Analysis of Clinker and Related Materials, in: Proceedings of the 5th International Conference on Cement Microscopy. pp. 1–10.

Awasthi, S., Fuerbach, A., Kane, D.M., 2021. Micro-volumetric analysis of complex fs laser processed sites using optical surface profilometry (OSP). Opt. Laser Technol. 140, 106997 https://doi.org/10.1016/j.optlastec.2021.106997.

Bourdillon, A.J., Self, P.G., Stobbs, W.M., 1981. Crystallographic orientation effects in energy dispersive X-ray analysis. Philos. Mag. A 44, 1335–1350. https://doi.org/10.1080/01418618108235813.

Chromy, S., 1967. High-temperature microscopic investigation of tricalcium silicate and dicalcium silicate phases in portland cement clinker. J. Am. Ceram. Soc. 50, 677–681. https://doi.org/10.1111/j.1151-2916.1967.tb15029.x.

Cross, S., Kreth, J., Wali, R.P., Sullivan, R., Shi, W., Gimzewski, J.K., 2009. Evaluation of bacteria-induced enamel demineralization using optical profilometry. Dent. Mater. 25, 1517–1526. https://doi.org/10.1016/j.dental.2009.07.012.

Ersoy, O., Aydar, E., Gourgaud, A., Bayhan, H., 2008. Quantitative analysis on volcanic ash surfaces: application of extended depth-of-field (focus) algorithm for light and scanning electron microscopy and 3D reconstruction. Micron 39, 128–136. https://doi.org/10.1016/j.micron.2006.11.010.

Evans, C.J., Paul, E., Dornfeld, D., Lucca, D.A., Byrne, G., Tricard, M., Klocke, F., Dambon, O., Mullany, B.A., 2003. Material removal mechanisms in lapping and polishing. CIRP Ann. - Manuf. Technol. 52, 611–633. https://doi.org/10.1016/S0007-8506(07)60207-8.

Famy, C., Brough, A.R., Taylor, H.F.W., 2003. The C-S-H gel of Portland cement mortars: Part I. The interpretation of energy-dispersive X-ray microanalyses from scanning electron microscopy, with some observations on C-S-H, AFm and AFt phase compositions. Cem. Concr. Res. 33, 1389–1398. https://doi.org/10.1016/S0008-8846(03)00064-4.

Famy, C., Scrivener, K.L., Crumbie, A.K., 2002. What causes differences of C-S-H gel grey levels in backscattered electron images? Cem. Concr. Res. 32, 1465–1471.

Fukuda, K., Maki, I, 1989. Orientation of β-Ca2SiO4 solid solution lamellae formed in the host α-phase. Cem. Concr. Res. 19, 913–918. https://doi.org/10.1016/0008-8846(89)90104-X.

Gauvin, R., 2012. What remains to be done to allow quantitative X-ray microanalysis performed with EDS to become a true characterization technique? (https://doi.org/DOI:). Microsc. Microanal. 18, 915–940. https://doi.org/10.1017/S1431927612001468.

Georget, F., Wilson, W., Scrivener, K.L., 2021. edxia: microstructure characterisation from quantified SEM-EDS hypermaps (https://doi.org/). Cem. Concr. Res. 141, 106327. https://doi.org/10.1016/j.cemconres.2020.106327.

Ghose, A., Barnes, P., 1979. Electron microprobe analysis of Portland cement clinkers. Cem. Concr. Res. 9, 747–755.

Ghose, A., Chopra, S., Young, J.F., 1983. Microstructural characterization of doped dicalcium silicate polymorphs. J. Mater. Sci. 18, 2905–2914.

Ghosh, S.N., Rao, P.B., Paul, A.K., Raina, K., 1979. Review - The chemistry of dicalcium silicate mineral. J. Mater. Sci. 14, 1554–1566.

Gross, S., 1977. The mineralogy of the Hatrurim Formation. Isr. Geol. Surv. Isr. Bull. 70, 1–80.

Harrisson, A.M., Taylor, H.F.W., Winter, N.B., 1985. Electron-optical analyses of the phases in a portland cement clinker, with some observations on the calculation of quantitative phase composition. Cem. Concr. Res. 15, 775–780.

Jupe, A.C., Wilkinson, A.P., Funkhouser, G.P., 2012. Simultaneous study of mechanical property development and early hydration chemistry in Portland cement slurries using X-ray diffraction and ultrasound reflection. Cem. Concr. Res. 42, 1166–1173. https://doi.org/10.1016/j.cemconres.2012.05.013.

Kang, K.W., Pereda, M.D., Canafoglia, M.E., Bilmes, P., Llorente, C., Bonetto, R., 2012. Uncertainty studies of topographical measurements on steel surface corrosion by 3D scanning electron microscopy. Micron 43, 387–395. https://doi.org/10.1016/j.micron.2011.10.005.

Kjellsen, K., Helsing Atlassi, E., 1998. X-ray microanalysis of hydrated cement: is the analysis total related to porosity? Cem. Concr. Res. 28, 161–165. https://doi.org/10.1016/S0008-8846(97)00201-9.

Kjellsen, K.O., Monsøy, A., Isachsen, K., Detwiler, R.J., 2003. Preparation of flat-polished specimens for SEM-backscattered electron imaging and X-ray microanalysis-importance of epoxy impregnation. Cem. Concr. Res. 33, 611–616.

Limandri, S., Galván Josa, V., Valentinuzzi, M.C., Chena, M.E., Castellano, G., 2016. 3D scanning electron microscopy applied to surface characterization of fluorosed dental enamel. Micron 84, 54–60. https://doi.org/10.1016/j.micron.2016.02.001.

Maimouni, H., Remond, S., Huchet, F., Richard, P., Thiery, V., Descantes, Y., 2018. Quantitative assessment of the saturation degree of model fine recycled concrete aggregates immersed in a filler or cement paste. Constr. Build. Mater. 175. https://doi.org/10.1016/j.conbuildmat.2018.04.211.

Maki, I., 2006a. Formation and microscopic textures of Portland cement clinker minerals. Part 1. Cem. Wapno, Bet. 65–85.

Maki, I., 2006b. Formation and microscopic textures of Portland cement clinker minerals. Part 2. Cem. Wapno, Bet. 135–158.

Marusin, S.L., 1995. Sample preparation - the key to SEM studies of failed concrete. Cem. Concr. Compos. 17, 311–318. https://doi.org/10.1016/0958-9465(95)00020-D.

Midgley, H.G., Bennet, M., 1971. A microprobe analysis of larnite and bredigite from Scawt Hill, Larne, Northern Ireland. Cem. Concr. Res. 1, 413–418.

Miller, M., Bobko, C., Vandamme, M., Ulm, F.-J., 2008. Surface roughness criteria for cement paste nanoindentation. Cem. Concr. Res. 38, 467–476. https://doi.org/10.1016/j.cemconres.2007.11.014.

Newbury, D.E., Ritchie, D.W.M., 2015. Performing elemental microanalysis with high accuracy and high precision by scanning electron microscopy/silicon drift detector energy-dispersive X-ray spectrometry (SEM/SDD-EDS). In: J. Mater. Sci, 50, pp. 493–518.

Newbury, D.E., Ritchie, N.W.M., 2013. Is scanning electron microscopy/energy dispersive X-ray spectrometry (SEM/EDS) quantitative? Scanning 35, 141–168. https://doi.org/10.1002/sca.21041.

Nowell, M.M., Witt, R.A., True, B.W., 2005. EBSD sample preparation: techniques, tips, and tricks. Micros. Today 13, 44–49.

Pacheco, J., Çopuroğlu, O., 2016. Quantitative energy-dispersive X-Ray microanalysis of chlorine in cement paste. J. Mater. Civ. Eng. 28 (1), 4015065.

Rayment, D.L., 1986. The electron microprobe analysis of the C-S-H phases in a 136 year old cement paste. Cem. Concr. Res. 16, 341–344. https://doi.org/10.1016/0008-8846(86)90109-2.

Rayment, D.L., Majumdar, A.J., 1994. Microanalysis of high-alumina cement clinker and hydrated HAC/SLAG mixtures. Cem. Concr. Res. 24, 335–342. https://doi.org/10.1016/0008-8846(94)90060-4.

Reed, S.J.B., 2005. Electron Microprobe Analysis and Scanning Electron Microscopy in Geology, Second edition.,. Cambridge University Press, Cambridge.

Rémond, G., Nockolds, C., Phillips, M., Roques-Carmes, C., 2006. Implications of polishing techniques in quantitative X-ray microanalysis. J. Res. Natl. Inst. Stand. Technol. 107, 639–662.

Richardson, I.G., Groves, G.W., 1993. Microstructure and microanalysis of hardened ordinary Portland cement pastes. J. Mater. Sci. 28, 265–277. https://doi.org/10.1007/BF00349061.

Ritchie, N.W.M., Newbury, D.E., Davis, J.M., 2012. EDS measurements of X-Ray intensity at WDS precision and accuracy using a silicon drift detector (https://doi.org/DOI:). Microsc. Microanal. 18, 892–904. https://doi.org/10.1017/S1431927612001109.

Rößler, C., Möser, B., Horst-Michael, L., 2017. 13. Characterization of microstructural properties of Portland cements by analytical scanning electron microscopy. De Gruyter.

Sargam, Y., Wang, K., 2021. Quantifying dispersion of nanosilica in hardened cement matrix using a novel SEM-EDS and image analysis-based methodology. Cem. Concr. Res. 147, 106524 https://doi.org/10.1016/j.cemconres.2021.106524.

Sarkar, S.L., Roy, D.M., 1985. Electron microprobe analyses of Nigerian clinkers. Cem. Concr. Res. 15, 662–668.

Scrivener, K., Bazzoni, A., Mota, B., Rossen, J.E., 2016. Electron microscopy, in: A Practical Guide to Microstructural Analysis of Cementitious Materials. pp. 351–415.

Scrivener, K.L., 2004. Backscattered electron imaging of cementitious microstructures: understanding and quantification. Cem. Concr. Compos. 26, 935–945.

Secco, M., Peruzzo, L., Palasse, L., Artioli, G., Viani, A., Gualtieri, A.F., 2014. Crystal chemistry of clinker relicts from aged cementitious materials. J. Appl. Crystallogr. 47, 1626–1637. https://doi.org/10.1107/S1600576714018287.

Setti, D., Kirsch, B., Aurich, J.C., 2019. Characterization of micro grinding tools using optical profilometry. Opt. Lasers Eng. 121, 150–155. https://doi.org/10.1016/j.optlaseng.2019.04.003.

Staněk, T., Sulovský, P., 2015. Active low-energy belite cement. Cem. Concr. Res. 68, 203–210. https://doi.org/10.1016/j.cemconres.2014.11.004.

Staněk, T., Sulovský, P., 2012. Dicalcium silicate doped with sulfur. Adv. Cem. Res. 24, 233–238. https://doi.org/10.1680/adcr.11.00021.

Stutzman, P., 2012. Microscopy of clinker and hydraulic cements. Rev. Mineral. Geochemistry 74, 101–146.

Stutzman, P., 2004. Scanning electron microscopy imaging of hydraulic cement microstructure. Cem. Concr. Compos. 26, 957–966.

Taylor, H.F.W., 1997. Cement Chemistry, 2nd edition,. T. Telford,, London.

Taylor, J.C., Aldridge, L.P., 1993. Full-profile rietveld quantitative XRD analysis of Portland cement: standard XRD profiles for the major phase tricalcium silicate (C3S: 3CaO.SiO2) (https://doi:/DOI:). Powder Diffr. 8, 138–144. https://doi.org/10.1017/S0885715600018054.

Velez, K., Maximilien, S., Damidot, D., Fantozzi, G., Sorrentino, F., 2001. Determination by nanoindentation of elastic modulus and hardness of pure constituents of Portland cement clinker. Cem. Concr. Res. 31, 555–561. https://doi.org/10.1016/S0008-8846(00)00505-6.

Wong, H.S., Buenfeld, N.R., 2006. Monte Carlo simulation of electron-solid interactions in cement-based materials. Cem. Concr. Res. 36, 1076–1082. https://doi.org/10.1016/j.cemconres.2006.03.006.

Yakowitz, H., 1968. Evaluation of Specimen Preparation and the Use of Standards in Electron Probe Microanalysis. In: Fifty Years of Progress in Metallographic Techniques, pp. 383–408.

Yamnova, N.A., Zubkova, N.V., Eremin, N.N., Zadov, A.E., Gazeev, V.M., 2011. Crystal structure of larnite b-Ca2SiO4 and specific features of polymorphic transitions in dicalcium orthosilicate. Crystallogr. Rep. 56, 210–220.

Yio, M.H.N., Wong, H.S., Buenfeld, N.R., 2016. 3D Monte Carlo simulation of backscattered electron signal variation across pore-solid boundaries in cement-based materials. Cem. Concr. Res. 89, 320–331. https://doi.org/10.1016/j.cemconres.2016.09.008.